Neurocomputing 358 (2019) 309–320

Contents lists available at ScienceDirect

Neurocomputing

journal homepage: www.elsevier.com/locate/neucom

Evolutionary prototype selection for multi-output regression

Mirosław Kordos [b], Álvar Arnaiz-González [a], César García-Osorio [a,*]

[a] Department of Civil Engineering, University of Burgos, Spain
[b] Department of Computer Science and Automatics, University of Bielsko-Biala, Poland

ARTICLE INFO

Article history:
Received 19 July 2018
Revised 5 March 2019
Accepted 23 May 2019
Available online 24 May 2019

Communicated by Prof. Zidong Wang

Keywords:
Prototype selection
Multi-output
Multi-target
Regression

ABSTRACT

A novel approach to prototype selection for multi-output regression data sets is presented. A multi-objective evolutionary algorithm is used to evaluate the selections using two criteria: training data set compression and prediction quality expressed in terms of root mean squared error. A multi-target regressor based on *k*-NN was used for that purpose during the training to evaluate the error, while the tests were performed using four different multi-target predictive models. The distance matrices used by the multi-target regressor were cached to accelerate operational performance. Multiple Pareto fronts were also used to prevent overfitting and to obtain a broader range of solutions, by using different probabilities in the initialization of populations and different evolutionary parameters in each one. The results obtained with the benchmark data sets showed that the proposed method greatly reduced data set size and, at the same time, improved the predictive capabilities of the multi-output regressors trained on the reduced data set.

1. Introduction

Machine Learning uses data sets for learning tasks, that consist of collections of observations and historical data. Each element of a data set is an instance that comprises a series of attributes: the input attributes that have to be measured for new observations; and, the output attributes that will be predicted. Traditionally, interest has mainly been focused on a single output attribute, which can either be nominal, for classification problems, or continuous for regression problems. Recent research has also focused on the simultaneous prediction of several target attributes. In this case, we refer to multi-label problems when considering nominal attributes [1], and we refer to multi-output regression problems when predicting continuous attributes [2].

1.1. Prototype selection

An important part of the Machine Learning pipeline is the initial data pre-processing step. Prototype selection (or instance selection) is one of the tasks at that stage. The first purpose of prototype selection is to obtain a reduced data set that can be used to train predictive models successfully with a similar performance to those that can be obtained using the whole data set [3]. In some cases, this reduction simply attempts to remove outliers and noisy instances, thereby facilitating the learning of a model and even improving its performance [4]. In others, the reduction is more aggressive, seeking the application of methods that might otherwise not be applied to the initial data set, and doing so without excessively affecting the performance of such methods. The availability of a reduced data set, that retains the properties of the original one, also permits several methods to be tested within a reasonable time, or to try several parameter values of a method to find the best model to solve the prediction task. Obviously, this task is much more challenging in multi-output regression than in single-label classification or in traditional (single-output) regression.

There are plenty of prototype selection methods for classification problems, for a thorough review of prototype selection methods, we recommend the taxonomy of Garcia et al. [5]. Over the past few years, some of these algorithms have been adapted to deal with regression problems [6,7]. It has also recently become possible to perform instance selection with extremely large data sets using algorithms of linear complexity [8] and implementations that exploit the parallelization of the map-reduce approach [9,10]. Unfortunately, there are only a few prototype selection methods for multi-label classification [11] and, to the best of our knowledge, there are as yet no prototype selection methods for multi-output regression. Thus, the aim of this paper is twofold:

* Corresponding author.
E-mail addresses: mkordos@ath.bielsko.pl (M. Kordos), alvarag@ubu.es (Á. Arnaiz-González), cgosorio@ubu.es (C. García-Osorio).

https://doi.org/10.1016/j.neucom.2019.05.055

- To propose the first prototype selection method that is capable of dealing with multi-output regression data sets (EPS-MOR). The method consists of several stages and uses the multi-objective evolutionary algorithm NSGA-II [12] as the engine that searches the solution space.
- To evaluate the performance of the EPS-MOR algorithm in an experimental study that thoroughly investigates the performance of the proposal, verifying not only the possibility of greatly reducing the size of the data sets, but also of improving the multi-output predictive capacity of the models trained with the reduced set.

The paper will be organized as follows: in Section 2, the concept of multi-output regression will be introduced; the instance selection task will be presented in Section 3 along with its aims and difficulties; in Section 4, the EPS-MOR algorithm is explained; then, the experimental setup and the results will be presented and analyzed in Section 5; finally, the main conclusions will be summarized in Section 6.

2. Multi-output regression

Multi-output regression, also known as multivariate or multi-target regression, is a task that involves the prediction of multiple continuous values by using a set of input variables or features [13] (so the problem is also multivariable). Consider a training set $D = \{(\mathbf{x}_1, \mathbf{y}_1), \ldots, (\mathbf{x}_n, \mathbf{y}_n)\}$ with n instances, each of them composed of d descriptive attributes and q target variables. Formally, a multi-target regression problem can be defined as the task of learning a model $h: \mathcal{X} \rightarrow \mathcal{Y}$, where $\mathcal{X} \subseteq \mathbb{R}^d$ is a set of input attributes, and $\mathcal{Y} \subseteq \mathbb{R}^q$ consists of a set of target variables that, given an unlabeled input instance $\mathbf{x}$, can predict its output set of variables [14,15].

A simple approach to multi-output regression would be to consider each of the outputs to be predicted as independent, and to learn a different model for each of them (commonly known as the single-target method). However, this procedure was incapable of exploiting the existing relationships between the different outputs. In fact, the models that exploit those relationships have proven that they can give much better results than those obtained by independent models [2,16,17]. Two strategies are commonly considered for dealing with multi-label/multi-output data sets: data transformation and algorithm adaptation [2]. The former is mainly based on transforming the multi-output label data set into a set of single-target data sets, which are then used for training a model for each target. The prediction is made by concatenating the different predictions of each regressor. In this work, we used four data-transformation methods implemented in Mulan [18]:

- Single-target regressor: the equivalent of the binary relevance method [19] for regression. Binary relevance creates as many single-label data sets as there are labels in the original multi-label data set. A classifier is then trained with each of these sets. Single-target regressors perform in the same way, but a regressor instead of a classifier is trained.
- Multi-target stacking: inspired by the stacked binary relevance technique, adapts the idea of stacked generalization [20] to multi-label learning. It consists of two stages: in the first stage, as many independent models as outputs are trained (as in single-target); these models are used to generate meta-variables for use at a later stage. The second stage builds the same number of models as the previous stage, but the original instances are augmented by the estimation of the values of their target attributes.
- Regressor chain: inspired by the classic classifier chains method [21]. Several regressors are chained in sequence, the first learns the relation between the inputs and the first output, the second uses the inputs and the output of the first to learn the second output,...: the last regression model attempts to predict the last output using all the inputs and all the outputs predicted by the previous regressors. The drawback of this method is that it is highly affected by the order in which the outputs are sorted in the chain.
- An ensemble of regressor chains serves to mitigate the influence of the order in the chaining order, by combining several regressor chains with different chaining orders in an ensemble.

3. Prototype selection and state-of-the-art

The task of selecting a subset of a large number of instances, examples or points, that are able to preserve the predictive capabilities of the entire set is an important and well-known problem in Machine Learning. These elements, that are able to summarize the whole data set, are called prototypes, representatives, or exemplars.

3.1. Prototype selection for single-label/output data

Prototype selection, also known as instance selection [5], is the task of selecting the most relevant instances/prototypes/examples from a data set. The aim of these algorithms is to obtain a subset of the original data set with the same (or in certain cases even higher) predictive capabilities than the original set [22]. In other words, given a training set, T, the problem is to select a subset $S \subseteq T$, so that S contains no irrelevant or superfluous instances, and so that the accuracy of a predictor trained with S is similar to the results of having used T [23] (or even better if the prototype selection method is capable of removing those instances that complicate the learning task, such as noise and anomalies).

Prototype selection is a multi-objective problem [24]: both accuracy and compression are important. A properly performed instance selection first removes noise and then compresses the remaining data. At the noise removal stage, both objectives can frequently be improved; removing the few noisy instances also lowers the *RMSE* and increases the compression. So, if the data set is more strongly compressed, improving compression worsen the *RMSE*, and the reverse.

The first prototype selection proposals for the nearest neighbor classifier date back to the late sixties and early seventies, where the two first methods, Condensed Nearest Neighbor [25] (CNN) and Edited Nearest Neighbour [26] (ENN), were proposed. Since then, a large number of different proposals have emerged. A detailed review of these methods is beyond the scope of the paper, although we recommend [5] to readers with an interest in those methods.

3.2. Subset representatives selection

The problem of finding a subset of representative examples that are able to summarize the whole data set has also been widely researched in such fields as computer vision, image processing, bioinformatics, and recommender systems, among others [27]. In these kinds of applications, the instances/examples are usually referred to as representatives or exemplars [28].

According to the type of information that representatives selection seeks, these algorithms can be divided into two groups. The first one assumes that data sets can be summarized with low-dimensional subspaces [29]. The algorithms of the second group use similarities/dissimilarities between pairs of instances instead of measurement vectors [30], which gives better results on high-dimensional data sets and makes possible to consider models beyond linear subspaces [28].

The problem of finding data representatives has been broadly researched [29,31]. Although, as for prototype selection, a thorough review of these methods is not the aim of this paper.

3.3. Evolutionary methods of prototype selection

Evolutionary algorithms make no assumptions about data set properties. Instead, they empirically verify large numbers of different subsets in an intelligent way to minimize the search in the solution space. This approach frequently yields much more efficient solutions than those that are achievable with non-evolutionary methods. Regarding prototype selection, evolutionary algorithms have shown better results than other approaches to the problem [32,33]. On the other hand, the good results usually imply much higher computational cost. Below, we briefly review the application of some evolutionary algorithms for instance selection for single-label classification tasks that can be found in the literature.

The first proposals of evolutionary instance selection methods were based on the application of conventional evolutionary search algorithms to the selection of prototypes [34,35]. Tolvi [36] used genetic algorithms for outlier detection and variable selection in linear regression models, performing both operations simultaneously. In [37], an algorithm called Cooperative Coevolutionary Instance Selection (CCIS) was presented. The method used two populations that were evolved cooperatively. The training set was divided into approximately N equal parts, and for each part a subpopulation of the first population was used. Each individual in a subpopulation encoded a subset of training instances. Likewise, each subpopulation was evolved using a standard genetic algorithm for its evolution. The second population consisted of combinations of instance sets. The population of individuals kept track of the best combinations of selectors for different subsets of instances, yielding a final selection that had the most promising combination for the whole data set.

Antonelli et al. [38] presented a complex genetic algorithm for dealing with prototype selection. They tackled the problem through a co-evolutionary approach in the framework of multi-objective evolutionary fuzzy systems. During the execution of the learning process, a genetic algorithm periodically evolved a population of reduced training sets. The single-objective algorithm aims to optimize an index that measures how close the results obtained with the reduced set are from those obtained when using the whole data set.

To the best of our knowledge, there are only three papers that describe the application of multi-objective evolutionary algorithms for prototype selection. All of them have been published in the last two years and were designed for single-label classification problems.

In [39], the MOEA/D algorithm was used to integrate instance selection, instance weighting, and feature weighting. The paper was focused on the use of co-evolution to approach the simultaneous selection of instances and hyper-parameters to train an SVM. The optimization criteria were the reduction of the training set and the performance (when the reduced set was used to train an SVM with the hyper-parameters found for the algorithm).

Another interesting approach is the one proposed by Escalante et al. [40], consisting in updating the training and validation partitions at each iteration of the genetic algorithm, in order to prevent the prototypes from overfitting a single validation data set.

In [41] Acampora et al. proposed a multi-objective training set selection. Their algorithm was mainly based on the evolutionary algorithm PESA-II [42] and was used for improving the performance of SVM by proper training set selection. They included several modification in their design for improving the performance of the PESA-II as a prototype selection algorithm.

Table 1 shows a comparison between the method proposed in this paper (EPS-MOR) and all the aforementioned algorithms.

3.4. Prototype selection for multi-output data

Even though prototype selection has been broadly researched for single-label classification and, to a lesser degree, for single-output regression; the same can not be said for multi-label/multi-output [11]. In the same way as classifier or regressor adaptation to multi-output, two approaches can be used for adapting single-label prototype selection methods to multi-output scenarios: data transformation (i.e. transform original multi-output data sets on one or more single-label data sets) and method adaptation (i.e. adapt the original single-label prototype selection methods, so that they can process multi-output data sets). Data transformation techniques for prototype selection were studied in [11]. Regarding method adaptation, there are currently only three prototype selection algorithms capable of processing multi-label data sets:

- Charte et al. [43] proposed a heuristic undersampling method for imbalanced multi-label data sets based on the canonical Wilson Editing method [26].
- Kanj et al. [44] proposed a prototype selection method, also based on Wilson Editing, that aims to purify the data set by removing harmful instances.
- Arnaiz-González et al. [45] recently proposed a method for adapting the local-set concept, successfully used on single-label instance selection methods [24,46], to multi-label data sets. It was used for adapting two single-label instance selection methods, LSSm and LSBo, to multi-label learning.

To the best of our knowledge, there are no prototype selection algorithms capable of processing multi-output regression data sets. So, up until now, it has not been possible to exploit the advantages offered by the prototype selection methods for this kind of problem: namely the speeding up of model learning, by means of data set size, and the performance increase of the trained models, as a consequence of the reduction of noisy and anomalous instances.

The challenges of prototype selection for multi-output data sets are manifold. One is related to the difficulties associated with prototype selection for regression [6] (it is usually difficult for the prototype selection algorithms for regression to improve the predictive capabilities of the methods trained with the selected subset [7]), and the other is related to the problems that arise when prototype selection is applied to multi-label data sets [43].

4. Evolutionary prototype selection for multi-output regression (EPS-MOR)

In this section, EPS-MOR, the proposed evolutionary method of prototype selection for multi-output regression is presented. The aim of EPS-MOR is to obtain several possible reduced training sets, which minimize two criteria: the training set size and the prediction error of a model trained on the reduced data set. Our method uses as a search algorithm a multi-objective genetic algorithm based on NSGA-II as a search algorithm to find the optimal solutions. The first criterion (compression) is just the ratio between the size of the selected subset and the size of the original set. The second criterion is the prediction error on the test set, which during the prototype selection process is approximated by the prediction error on the training set, because the output values of the test set instances are normally unknown just before the training starts.

Some characteristics of EPS-MOR worth highlighting are:

- For the first time, a prototype selection for multi-output regression is presented.
- Use of multi-parent multi-point crossover with optimized numbers of splits and parents.

Table 1
Comparison between the proposed method and several evolutionary instance selection algorithms. For each method the table shows the type of data set to which is applied (single-label or multi-output), the type of function is optimizing (single-objective or bi-objective), the evolutionary algorithm used for the search, the type of crossover and mutation operators, and if it uses Pareto fronts, how they are used.

Algorithm	Label	Objective	Evol. algorithm	Crossover	Mutation	Pareto front
CHC [35]	Single-label	Single-objective	CHC	Single-point	-	-
GGA [34]	Single-label	Single-objective	-	Single-point	Symmetric	-
CCIS [37]	Single-label	Single-objective	-	Two-point	Symmetric	-
Tolvi [36]	Single-output	Single-objective	-	Single-point	Symmetric	-
PAES-SOGA [38]	Single-output	Single-objective	(2+2)M-PAES	Single-point	Symmetric	-
EMOMIS [39]	Single-label	Bi-objective	MOEA/D	Single-point	Symmetric	*Ensemble* combination
MOPG [40]	Single-label	Bi-objective	NSGA-II	Multi-point	Symmetric	Highest accuracy
Pareto-TSS [41]	Single-label	Bi-objective	PESA-II	Single-point	Asymmetric	Sum model
EPS-MOR	Multi-output	Bi-objective	NSGA-II	Multi-point	Asymmetric	3-front combination

- Use of up to three populations with different initialization and mutation probabilities. These three can be merged into a single Pareto front, in order to reduce overfitting and improve coverage of the solution space.
- Use of asymmetric mutation: making it possible to have data sets with lower error in the populations.
- Efficient evaluation of the fitness function by pre-calculating and reusing the distances matrices for k-NN (calculated and sorted only once at the beginning of the process).

In the following sections more details are given of certain relevant steps of the method.

4.1. Basic concepts of evolutionary prototype selection

Prototype selection is a bi-objective task with two goals: minimization of the number of instances in the training set (compression) and maximization of the prediction quality of the model trained on the selected instances [24]. In the case of the regression task, the prediction quality is commonly measured by using the mean squared error on the test set.

Each individual in the population represents a set of selected instances. Every single position in the individual chromosome represents an instance of the training data set. A value of 1 at a given position means that the corresponding instance is selected and a value of 0 means that is rejected.

In standard (single-objective) genetic algorithms used for prototype selection, both objectives are incorporated into a single fitness function, which measures the quality of the obtained solution. One of the simplest versions of a fitness function is shown in Eq. (1):

$$fitness = \left(\gamma \frac{avgRMSE}{rmse} + (1-\gamma)\frac{avgNumInstances}{numInstances}\right)^{p} \quad (1)$$

where, the *RMSE* is the root mean square error of the model trained on the current training set, *avgRMSE* is the average *RMSE* over the whole population of training sets, *numInstances* is the number of selected instances in the current training set, and *avgNumInstances* is the average number of selected instances over the whole population of training sets. γ is a value between 0 and 1 that controls the importance given to each of the objectives. p is a positive real number, controlling the steepness of the fitness functions, i.e. how much the better solutions are favored.

As may be deduced, the most time-consuming part of the genetic algorithm is the evaluation of the fitness function value, as it requires a calculation of the *RMSE* performed by the predictive model on the training set. (In the method that is presented, special effort was spent on reducing this time, as will be discussed later.)

There are two problems with the single-objective approach. First, we must know which weights to assign to each criterion. Second, if we need several solutions with different weights, then the optimization needs to be run several times: each time with a different γ value (Eq. (1)) to achieve one solution, which is definitely a time-consuming process.

4.2. Multi-objective genetic algorithms for prototype selection

The main advantage of multi-objective evolutionary algorithms is that they do not require the coefficients that indicate the expected balance between the objectives (γ value of Eq. (1)) to be determined. Instead, these algorithms produce a set of solutions that generate the highest fitness, i.e. the result of the algorithm is the front of the non-dominated individuals (Pareto front) with different trade-offs between objectives. Solutions based on Pareto-front and domination between individuals [47] can be divided into ranking, elitist and diversity maintaining methods [48].

A solution $\mathbf{x}$ dominates another solution $\mathbf{y}$ (with the minimization goal) if it achieves better (lower) or equal values of all objective functions (of all criteria), and additionally better value of at least one objective function (one criterion) [49], this is when both equations below are satisfied:

$$\begin{cases} obj_i(\mathbf{x}) \le obj_i(\mathbf{y}) & \text{for} \quad \text{all } i \\ obj_i(\mathbf{x}) < obj_i(\mathbf{y}) & \text{for} \quad \text{at least one } i \end{cases} \quad (2)$$

where i is the objective function index ($i = 1 \ldots O$), O is the number of objectives, and $obj_i(...)$ is the objective function. The examples of domination between individuals and the Pareto front can be seen in Fig. 2.

Despite the fact that several multi-objective evolutionary algorithms have been proposed [12], the NSGA-II algorithm is the most frequently used and one of the best for bi-objective problems. (For more than two objetives, there is an extension of the aforementioned algorithm called NSGA-III [50]).

4.3. Genetic operators

Seeking to obtain the best results for the prototype selection problem, several improvements to the genetic operators were introduced, as explained below.

4.3.1. Crossover

There are two commonly used crossover schemes: single-point and many-point split. The former takes two parents and randomly determines one split point. The child inherits the first part of the chromosome from the first parent, and the second part from the second parent. Instead of a single-point split, many can be used, so the offspring is formed combining multiple parts of its two parents. Also, instead of two parents, the new individual can be obtained by combining several parts of multiple parents. In the method proposed in this paper, multi-point multi-parent crossover was used, since for the prototype selection task, a significant improvement of the convergence was observed. Nevertheless, using too many split points may not allow the genetic algorithm to build

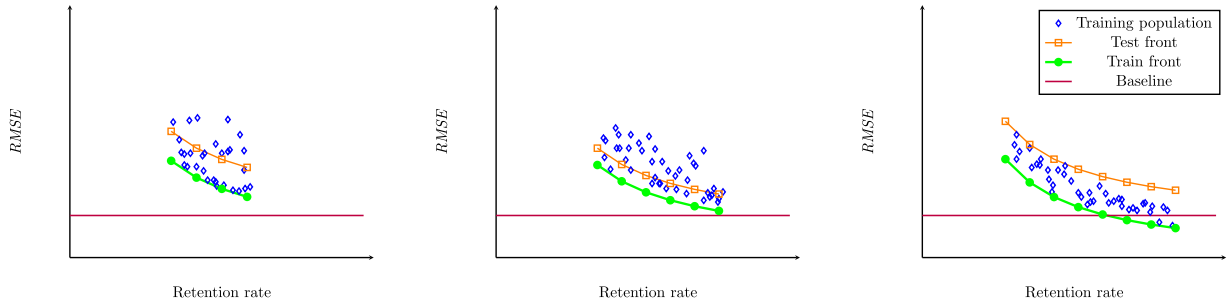

(a) Initial population (b) The front extends (c) Overfitting

Fig. 1. Formation of a single Pareto front during the prototype selection process.

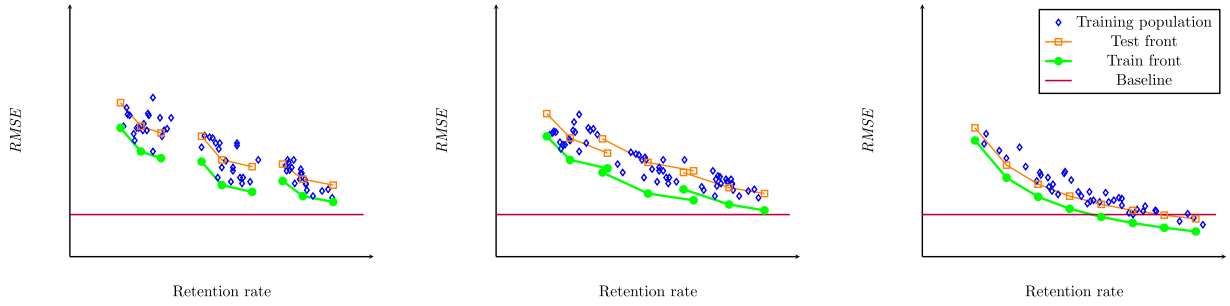

(a) Initial population (b) The fronts extend (c) No overfitting

Fig. 2. Formation of a Pareto front using three sub-fronts during the prototype selection process.

effectively the highly fitted blocks in the chromosome, as their construction will be permanently disrupted. Experimentally, we derived the formula shown in Eq. (3), explained later at the end of Section 5.2.

4.3.2. Mutation

There are cases where a genetic algorithm can find the optimal solutions even without the mutation operator. For example, when the chromosome is short enough and the population is large enough. However, in other cases the mutation operator is crucial, especially in the final stages of the process, where the diversity of the population is limited and some optimal positions in the chromosome may no longer exist in any individual. (Or even if they do exist, the individual may have low fitness and therefore a low probability of selection as a parent for the next generation.)

Commonly, in evolutionary algorithms, a symmetric mutation operator is used, i.e. the probability of switching from 1 to 0 is the same as from 0 to 1. The problem that arises is that symmetric mutation exerts a pressure on the process to set, on average, the same number of ones and zeros as in the initial population. That problem is also one of the reasons why the multi-objective prototype selection genetic algorithms tend to contract the Pareto front, not including the solutions that have selected either very few or too many instances.

In the problem of prototype selection, we are not interested in extreme data set reduction, if it is at the cost of worsening the error too much (which will make the selection useless in real applications, as the subset would not be representative of the original data set, leaving it of no use for learning tasks). We are interested in reductions that keep the statistical properties of the original data set, but allowing predictors with lower errors and good generalization to be obtained.

In some data sets, the lowest error is obtained when quite a lot of instances are rejected, say 40% or 50%. In that case, there is no problem and the symmetric mutation will do properly. Nonetheless, for other data sets obtaining the lowest error requires rejecting very few instances, frequently below 10%. In these cases, we should enforce those solutions will be found by generating the initial population with much more ones than zeros in the chromosome and using the asymmetrical mutation operator to maintain this proportion as the process progresses. Thus, for example the probability of switching from 0 to 1 can be 90%, while the probability of switching from 1 to 0 will be 10%.

4.4. Extending the Pareto front

In a typical optimization process, where the genetic algorithm directly optimizes the final objectives, a simple approach to find the best possible solution is to increase the number of iterations. Nevertheless, prototype selection belongs to a different class of problems, because the optimization is performed on the training set (the test set is unknown during the optimization), yet one of the objectives is to reduce the *RMSE* in the test. For this reason, the *RMSE* on the training set is minimized during prototype selection, assuming that it yields a decrease of the *RMSE* on the test set.

It is similar to the process of training a predictive model. Analogously, as we cannot train the model for too many iterations, we cannot run the genetic optimization too long, because overfitting begins to occur at a certain point; the *RMSE* is constantly decreasing on the training set, but at a certain point it begins to increase in the test set. The simplest solution to this problem is to use early stopping, which in our preliminary experiments worked well in more than half of the data sets.

For explanatory purposes, let us consider the idealized situation shown in Figs. 1 and 2. At the beginning of the optimization, all positions in all chromosomes have random values. Thus, the locations of all the individuals[1] in the compression-*RMSE* space are

[1] Each individual representing the instances selected from the original data set.

very close to each other and they all have a relatively poorly balanced compression-*RMSE* for any γ value in Eq. (1). These locations are shown in Fig. 1 (a), where the blue diamonds represent the solutions of the evolutionary algorithm. Each solution (set of selected instances) on the Pareto front of the training set is used to train a model. The green circles (connected with the thick line) represent the *RMSE* value obtained from the regressor that was in turn trained using the selected subset applied to the training subset itself. Obviously, this *RMSE* is a very optimistic estimation of the error as the same data set is used both for training and testing. The result of the model on the test set is expected to be higher and, in the figures, it is represented by an orange square just above the green circle (both marks: the orange square and the green circle are obtained from the same training set of selected instances, hence they have the same compression value — the compression of the selected training set). As the green circles, the orange squares are connected by a line, although this time a thin one that represents the expected Pareto front on testing. The baseline represented by the horizontal line is the *RMSE* on the training set obtained by the regressor trained on the original full size data set.

As the optimization progresses, the points move gradually to the positions shown in Fig. 1 (b), and then 1 (c). But, before they reach the positions in Fig. 1 (c), the overfitting has already started to happen (the green thick line in Fig. 1 (c) is lower than in Fig. 1 (b), and the thin orange line is situated at a higher point, i.e. more *RMSE*).

Nonetheless, as shown in Fig. 2 (c), when there are more fronts, solutions with low compression and low *RMSE* are reached before overfitting occurs. (The thick green line in Fig. 2 (c) is lower than in Fig. 2 (b), and the thin orange line is also lower).

Frequently we do not need the front to be extended in the direction of low compression (high retention rate), because the lowest *RMSE* is already reached below the baseline in Fig. 1 (b) and will probably not improve any further. However, if the lowest *RMSE* is at or above the baseline, we may want to search for a solution with an even lower *RMSE*. Running the optimization for more iterations will not always lower the *RMSE*, as it will also cause overfitting. We therefore need to obtain more fronts, which we call sub-fronts, to cover a broader space without overfitting. The subfronts are obtained by generating the initial populations with different proportions of 0 and 1, and then, using different probabilities in the mutation phase, so that the percentage of 0s and 1s in the chromosomes remain relatively close to the proportions in the initial populations, as it is shown in Fig. 2 (a). Finally, the subfronts will be merged into one Pareto front (and thus some points from some sub-front may not be included in the final front, if the points from another sub-front satisfy both objectives with greater accuracy).

4.5. Summary of EPS-MOR

In summary, the sequence of steps of the proposed method is:

1. Calculate and sort the distance matrices that will be used later by *k*-NN based predictive models.
2. Obtain the Pareto front of the selected test sets:
   (a) Initialize the population *P* with *S* individuals, with different proportions of 0s and 1s in each front.
   (b) Start the iterative prototype selection process:
      i. Evaluate the population *P* according to the two objectives: compression and average *RMSE*.
      ii. Select the individuals that will be included in each of the fronts. First, the non-dominated individuals from *P* populations are transferred to the first front. Then, the next front is selected from remaining individuals. This process performance is optimized by Fast Non-dominated Sort (for further details see [12]).
      iii. Calculate crowding distances. Within each front a crowding distance for each individual is calculated (for further details see [12]). It determines the distance between neighboring individuals from a given front and promotes more diverse solutions in the following selection process.
      iv. Apply the multi-point multi-parent crossover. In this step a population P' with *s* children is created. For each child, a number of parents is chosen using ranking selection (using values specific to each front and then crowding distance — individuals with smaller values are selected).
      v. Apply the mutation operator with probabilities specific to each front.
      vi. Merge the populations. Populations *P* and P' are merged into a single one ($P = P \cup P'$).
      vii. Select the individuals that will be included in the combined front and calculate the crowding distances for the merged population *P*.
      viii. From the population *P* (with size $2 \cdot s$) *s* best individuals are selected. In this selection, the individuals from the front are prioritized. If the front has less than *s* individuals, all of them are included and the rest, up to *s*, are randomly selected from the rest of individuals of population *P* not in the front. If in the front there are already more than *s* individuals, only the *s* with largest crowding distance are selected.
      ix. Evaluate the stopping criterion. The algorithm stops if the criterion is met, otherwise the algorithm will perform the next iteration.
   (c) Return, as the result of the prototype selection process, the first front of non-dominated solutions with all the solutions found (each of them represents a reduced data set).
3. Check whether the next front is required: if so, go to point 2a.
4. Merge all fronts into one final front of solutions.

5. Experimental evaluation

The performance of EPS-MOR was experimentally evaluated in a 10-fold cross-validation process using several multi-output regressors and compared with the results of training the regressors using the original data sets. The software was written in C# language for performing the prototype selection process, and Mulan [18] was used to evaluate the results. The experiments were performed on the 13 multi-output regression data sets (see Table 2) that are the benchmark files available from the Mulan project website[2]. All the

Table 2
Summary of data sets characteristics: name, domain, number of instances, features, and targets.

Data sets	Domain	Instances	Attributes		Targets
			Num.	Nom.	
Andromeda	Water	49	30	0	6
Slump	Concrete	103	7	0	3
EDM	Machining	154	16	0	2
ATP7D	Forecast	296	211	0	6
Solar flare 1	Forecast	323	0	10	3
ATP1D	Forecast	337	411	0	6
Jura	Geology	359	15	0	3
Online sales	Forecast	639	401	0	12
ENB	Buildings	768	8	0	2
Water quality	Biology	1 060	14	0	16
Solar flare 2	Forecast	1 066	0	10	3
SCPF	Forecast	1 137	23	0	3
River flow 1	Forecast	9 125	64	0	8

[2] Available at http://mulan.sourceforge.net/datasets-mtr.html.

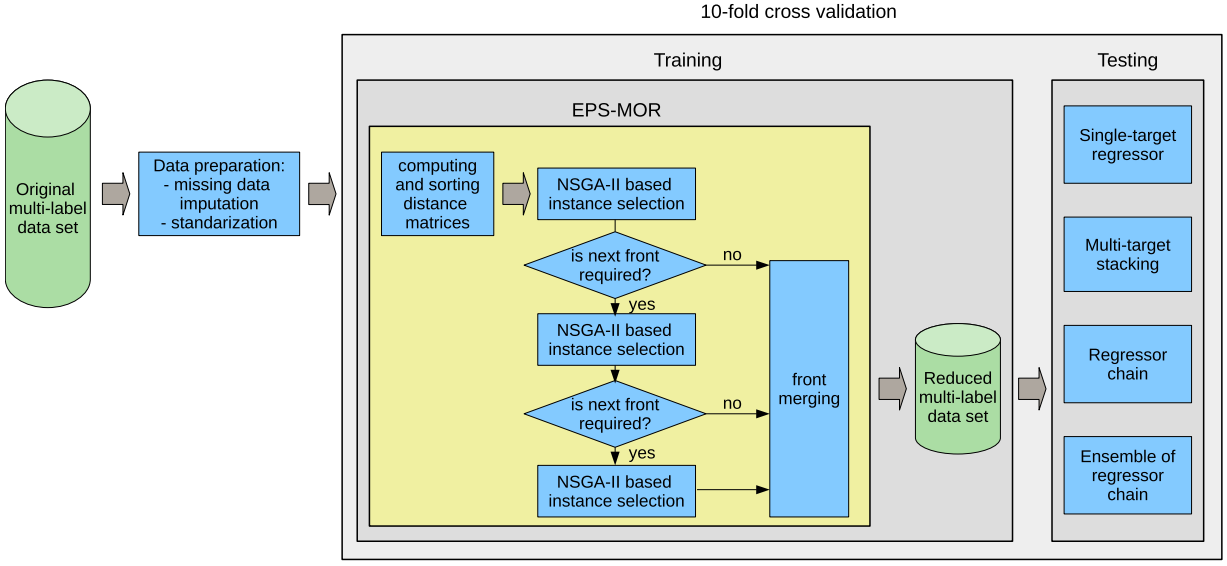

Fig. 3. The graphical representation of the experimental process.

software and data sets used in the experiments can be downloaded from http://kordos.com/eps-mor.

5.1. Experimental setup

The experimental setup is presented in Fig. 3. First of all, two additional pre-processing steps were performed: missing data imputation (replacing missing values by the mean of the feature), and nominal attribute replacement (transforming them into binary ones)[3].

During training, the distance matrices were firstly computed and sorted. Then the NGSA-II algorithm was used for searching the solution space. Initially, the population was randomly generated with a 0.5 probability of 0 and 1 at each position, equal to the probability of either selecting or rejecting each instance (if needed, the next two sub-fronts were obtained, with different proportions of 0s and 1s, and all the sub-fronts merged into the final Pareto front).

In the testing part, the base regressor was k-NN ($k = 1, 3, 5$) adapted to multi-output regression by four different techniques [14]: single-target regressor, multi-target stacking, regressor chain, and ensemble of regressor chains. All of the parameters of the regressors were set to the default values in Mulan. The average root mean squared error (*RMSE*) was used as a measure of the prediction quality:

$$RMSE = \frac{1}{q}\sum_{j=1}^{q}\sqrt{\frac{\sum_{i=1}^{n}\left(y_{ij}-\hat{y}_{ij}\right)^2}{n}}$$

where, n is the number of instances, q the number of outputs, y_i and $\hat{y}_i$ are, respectively, the vector of the actual and the predicted outputs for $\mathbf{x}_i$.

In a typical case, Fig. 4 shows the Pareto front obtained in training (green circles), some of the solutions of this front (orange squares) and their positions in testing, and a horizontal line representing the error obtained by the regressor trained with the whole data set. As can be seen, the solutions that find themselves exactly on the Pareto front in training are displaced when the testing error is considered (although their compression is exactly the same, their *RMSE* can differ). However, it is expected that most of them will be close enough to the ideal Pareto front in testing (some exceptions are mentioned in the discussion of the experiments).

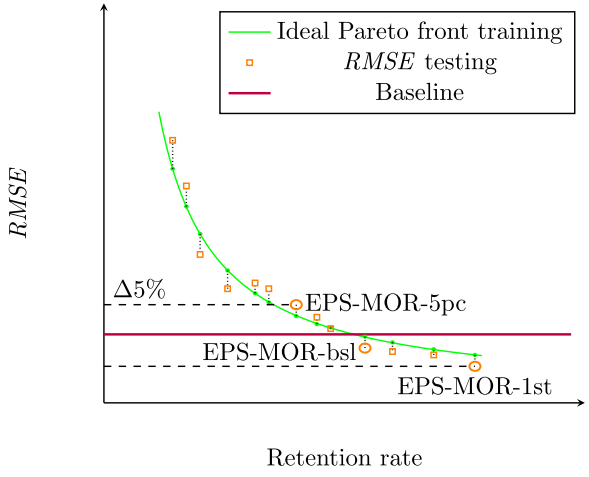

Fig. 4. Schematic representation of the different instance selection solutions selected for the experimental comparisons. Baseline represents the *RMSE* obtained with the test set of the regressor trained on the original training data set.

The results of a multi-objective evolutionary algorithm simultaneously yield several solutions. These results are always advantageous, since one could then either choose solutions with higher compression, or solutions with a lower error, depending on the specific needs of the problem to solve (as discussed later on, the high cost, traditionally associated with genetic algorithms, is not so high, if they are carefully implemented). Nevertheless, to facilitate the analysis of the experimental results, only 3 representative solutions were considered:

- EPS-MOR-1st: The first point of the Pareto Front, i.e., the solution with the lowest compression and with the lowest *RMSE* on the training set. Although it is not guaranteed that this subset will produce the lowest *RMSE* on the training set in every case, it will usually do so.
- EPS-MOR-bsl: The point of the Pareto front when the front intersects the baseline on the test set (we understand the baseline to be the *RMSE* obtained on the test set with the

[3] Both the missing data imputation and nominal to binary features replacement were performed by using Weka [51].

Table 3
Summary of the parameters' values of EPS-MOR used in the experiments.

Parameter	Value
Number of epochs	25
Number of individuals	96
Number of parents and crossover points	given by Eq. (3)
Initialization probability	0.5 (1st front), 0.8 (2nd front), 0.92 (3rd front)
Mutation probability (1st front)	0.005 from 1 to 0 and from 0 to 1
Mutation probability (2nd front)	0.002 from 1 to 0 and 0.008 from 0 to 1
Mutation probability (3rd front)	0.001 from 1 to 0 and 0.009 from 0 to 1
Crossover probability	100%
Inner regressor	set of single target *k*-NN regressors

Table 4
Summary of the results for the *RMSE* with *k*-NN regressor with $k = 1$ (lower is better). The best result for each data set (and regressor) and the best values are highlighted in bold.

(a) single-target

Data set	Original	EPS-MOR		
		1st	bsl	5pc
Andromeda	0.4478	**0.4419**	**0.4419**	0.5151
SCPF	0.9580	**0.7633**	0.8556	0.8556
Water quality	0.9421	**0.8944**	0.9036	0.9036
Solar flare 1	1.2250	**0.8985**	1.1894	1.2981
Solar flare 2	0.9353	**0.8396**	0.9193	0.9557
Slump	0.9086	**0.8031**	0.8857	0.9468
ATP1D	0.5535	0.5151	**0.4872**	0.6966
ATP7D	0.7823	**0.7342**	0.7412	0.7844
EDM	0.6035	**0.5252**	0.5970	0.6718
River flow 1	0.0901	**0.0661**	0.0786	0.0786
ENB	0.5732	0.5257	**0.4443**	**0.4443**
Jura	0.8133	**0.8059**	**0.8059**	0.8577
Online sales	0.9003	**0.8589**	0.8956	0.9637
Average	0.7487	**0.6671**	0.7112	0.7671

(b) stacking of single-target

Data set	Original	EPS-MOR		
		1st	bsl	5pc
Andromeda	0.4478	**0.4419**	**0.4419**	0.5151
SCPF	0.9580	**0.7633**	0.8556	0.8556
Water quality	0.9421	**0.8944**	0.9036	0.9036
Solar flare 1	1.2312	**0.8988**	1.1832	1.2923
Solar flare 2	0.9506	**0.8389**	0.9203	0.9558
Slump	0.9086	**0.8031**	0.8857	0.9468
ATP1D	0.5535	0.5151	**0.4872**	0.6966
ATP7D	0.7823	**0.7342**	0.7412	0.7844
EDM	0.6035	**0.5252**	0.5970	0.6718
River flow 1	0.0901	**0.0661**	0.0786	0.0786
ENB	0.5732	0.5257	**0.4443**	**0.4443**
Jura	0.8133	**0.8059**	**0.8059**	0.8577
Online sales	0.9003	**0.8589**	0.8956	0.9637
Average	0.7503	**0.6670**	0.7108	0.7666

(c) chain of *k*-NN regressors

Data set	Original	EPS-MOR		
		1st	bsl	5pc
Andromeda	0.4478	**0.4419**	**0.4419**	0.5151
SCPF	0.9580	**0.7633**	0.8556	0.8556
Water quality	0.9421	**0.8944**	0.9036	0.9036
Solar flare 1	1.2525	**0.8976**	1.1832	1.2959
Solar flare 2	0.9799	**0.8387**	0.9193	0.9549
Slump	0.9086	**0.8031**	0.8857	0.9468
ATP1D	0.5535	0.5151	**0.4872**	0.6966
ATP7D	0.7823	**0.7342**	0.7412	0.7844
EDM	0.6035	**0.5252**	0.5970	0.6718
River flow 1	0.0901	**0.0661**	0.0786	0.0786
ENB	0.5732	0.5257	**0.4443**	**0.4443**
Jura	0.8133	**0.8059**	**0.8059**	0.8577
Online sales	0.9003	**0.8589**	0.8956	0.9637
Average	0.7542	**0.6669**	0.7107	0.7668

(d) ensemble of chains

Data set	Original	EPS-MOR		
		1st	bsl	5pc
Andromeda	**0.4114**	0.4912	0.4912	0.5555
SCPF	0.8266	**0.7453**	0.7938	0.7938
Water quality	0.8284	**0.7983**	0.8138	0.8138
Solar flare 1	1.1081	**0.8928**	1.0540	1.1344
Solar flare 2	0.9234	**0.8164**	0.8776	0.8831
Slump	**0.7516**	0.7861	0.8507	0.9070
ATP1D	**0.4772**	0.5555	0.5330	0.6893
ATP7D	0.6810	**0.6702**	0.7035	0.7051
EDM	0.5804	**0.5228**	0.6146	0.7409
River flow 1	0.0837	**0.0659**	0.0784	0.0784
ENB	0.4623	0.4175	**0.3883**	**0.3883**
Jura	**0.7304**	0.7431	0.7431	0.8020
Online sales	0.7907	**0.7786**	0.8086	0.8781
Average	0.6658	**0.6372**	0.6731	0.7207

regressor trained on the whole training set). This result would usually correspond to a solution with a *RMSE* that is close to the one obtained with the whole data set, but with higher compression than EPS-MOR-1st.

- EPS-MOR-5pc: The point of the Pareto front that shows a 5% higher *RMSE* on the test set than the first solution (EPS-MOR-1st). That solution has a worse *RMSE*, but with much more compression than EPS-MOR-1st.

At times, some of the solutions can actually be the same: for example, if the first point is above the baseline, EPS-MOR-1st and EPS-MOR-bsl share the same *RMSE*. It is also possible that EPS-MOR-5pc might have a lower error than, for example, the error of the EPS-MOR-1st plus 5%, if the last point of the Pareto front is reached and its error is still not 5% higher than EPS-MOR-1st. Even in some cases, the first point of the Pareto front has higher error than some of the next points and EPS-MOR-bsl could be even better than EPS-MOR-1st, for some data sets.

5.2. Parameters of the evolutionary prototype selection algorithm

An initial exploratory analysis was performed before the experiments, in order to select the best parameters for EPS-MOR. Despite the fact that a carefully and customized parameter tuning for each data set could have achieved better results, we launched all the experiments with a common configuration of parameters for all data sets. Table 3 shows the values of the parameters finally used, which are explained in greater detail below.

- Initialization: the initial probability in the first Pareto front was that the chromosomes of the individuals would have a value of 1 in a position is 0.5. This probability increased to 0.8 for the individuals in the second Pareto front (if needed), and to 0.92 for the individuals in the third Pareto front (if needed). Nevertheless, the first Pareto front was sufficient in 59% of our experiments, as the *RMSE* obtained with it was already below 95% of the baseline and the inclusion of additional fronts did not reduce the *RMSE* any further.

Table 5
Summary of the results for the *RMSE* with *k*-NN regressor with $k = 3$ (lower is better). The best result for each data set (and regressor) and the best values are highlighted in bold.

(a) Single-target

Data set	Original	EPS-MOR		
		1st	bsl	5pc
Andromeda	0.5870	**0.5066**	0.5810	0.6491
SCPF	0.8430	**0.7366**	0.8224	0.8646
Water quality	0.7884	0.7804	**0.7770**	0.8103
Solar flare 1	1.0279	**0.9096**	0.9897	0.9897
Solar flare 2	0.9072	**0.8592**	0.8772	0.8772
Slump	**0.7000**	0.7398	0.7398	0.7694
ATP1D	**0.4389**	0.4577	0.4577	0.4698
ATP7D	**0.6268**	0.6360	0.6360	0.6643
EDM	0.5866	**0.5833**	**0.5833**	0.6190
River flow 1	0.0929	**0.0717**	0.0744	0.0744
ENB	**0.2967**	0.3049	0.3049	0.3117
Jura	**0.7229**	0.7273	0.7273	0.7713
Online sales	**0.8001**	0.8199	0.8199	0.8938
Average	0.6476	**0.6256**	0.6454	0.6742

(b) Stacking of single-target

Data set	Original	EPS-MOR		
		1st	bsl	5pc
Andromeda	0.5642	**0.4663**	0.5659	0.6078
SCPF	0.8578	**0.7356**	0.8232	0.8650
Water quality	0.7878	0.7853	**0.7841**	0.8356
Solar flare 1	1.0607	**0.9086**	0.9871	0.9871
Solar flare 2	0.9056	**0.8684**	0.8886	0.8886
Slump	**0.6868**	0.7708	0.7708	0.7793
ATP1D	**0.4391**	0.4580	0.4580	0.4702
ATP7D	**0.6268**	0.6361	0.6361	0.6644
EDM	**0.5715**	0.5806	0.5806	0.6165
River flow 1	0.0934	**0.0728**	0.0756	0.0756
ENB	**0.2764**	0.2965	0.2965	0.3039
Jura	**0.7350**	0.7385	0.7385	0.7739
Online sales	**0.7983**	0.8240	0.8240	0.9016
Average	0.6464	**0.6263**	0.6484	0.6746

(c) chain of *k*-NN regressors

Data set	Original	EPS-MOR		
		1st	bsl	5pc
Andromeda	0.5700	**0.4976**	0.5915	0.6409
SCPF	0.8333	**0.7356**	0.8188	0.8620
Water quality	0.7890	0.7871	**0.7846**	0.8074
Solar flare 1	1.0187	**0.9106**	0.9824	0.9824
Solar flare 2	0.8876	**0.8593**	0.8858	0.8858
Slump	**0.7209**	0.7508	0.7508	0.7786
ATP1D	**0.4372**	0.4577	0.4577	0.4695
ATP7D	**0.6243**	0.6343	0.6343	0.6608
EDM	**0.5749**	0.5833	0.5833	0.6107
River flow 1	0.0930	**0.0719**	0.0749	0.0749
ENB	**0.2919**	0.3089	0.3089	0.3187
Jura	0.7293	**0.7239**	**0.7239**	0.7733
Online sales	**0.7943**	0.8151	0.8151	0.8960
Average	0.6434	**0.6258**	0.6471	0.6739

(d) ensemble of chains

Data set	Original	EPS-MOR		
		1st	bsl	5pc
Andromeda	0.5999	**0.5285**	0.6112	0.6620
SCPF	0.7763	**0.7370**	0.7862	0.8181
Water quality	0.7654	**0.7653**	0.7689	0.7945
Solar flare 1	1.0129	**0.8924**	0.9241	0.9241
Solar flare 2	0.9149	**0.8517**	0.8606	0.8606
Slump	**0.7166**	0.7249	0.7249	0.7588
ATP1D	**0.4315**	0.4449	0.4449	0.4659
ATP7D	0.6083	**0.6066**	**0.6066**	0.6232
EDM	0.6278	**0.6161**	**0.6161**	0.6773
River flow 1	0.0757	**0.0740**	0.0776	0.0776
ENB	0.3438	**0.3253**	**0.3253**	0.3499
Jura	**0.7247**	0.7270	0.7270	0.7749
Online sales	**0.7780**	0.7824	0.7824	0.8874
Average	0.6443	**0.6212**	0.6351	0.6673

- Population size: the optimal value slightly grows with the chromosome length, and it was about 60–70 for the data sets with less than 1 000 instances and around 75–85 for the larger ones. The difference in the optimization time, between 65 and 100 individuals, was about 3% – the function resembled a parabolic curve and grew very slowly close to the minimum (a very flat parabola). Using only a single CPU, the time of the process is proportional to the number of fitness function evaluations. Nonetheless, in multi-CPU solutions, the dependence is more complex and for optimal performance the population size should be a multiple of the available CPU core number. As we used a 48-core machine for the experiments, we set the population size at 96 individuals.
- Crossover: multi-point multi-parent crossover can significantly increases the convergence on the genetic instance selection algorithm (a 3-fold increase in our experiments). The optimal number of parents can be equal to the optimal number of split points and both can be set, so on average the split occurs from every 10 positions for short chromosomes up to every 100 positions for longer chromosomes (Eq. (3)). The parents were randomly selected with a probability proportional to their fitness value. Each selection was independent, so it could happen that one parent was selected more than once, giving its genetic material to more than one segment of the child chromosome.

$$M = \begin{cases} round(n/10) & \text{for} \quad n \le 1\,000 \\ 100 + round((n - 1000)/100) & \text{for} \quad n > 1\,000 \end{cases} \tag{3}$$

5.3. Results and discussion

Tables 4, 5, and 6 show the *RMSE* results of the *k*-NN classifier ($k = 1, 3, 5$) adapted to multi-label by means of: single target, multi-target stacking, chain of *k*-NN, and an ensemble of *k*-NN chains, with (EPS-MOR-1st, EPS-MOR-5p, EPS-MOR-bsl) and without prototype selection. Table 7 shows the compression rates (in percentages) achieved by EPS-MOR.

As shown in Tables 4, 5, 6 (a), the application of some data set size reduction algorithm (EPS-MOR-1st solutions) reduced the *RMSE* consistently in most data sets, as might be expected, given that prototype selection was very likely to remove outliers and noisy instances. The compression achieved by EPS-MOR-1st was remarkable, at around 40%, i.e. the 60% of instances were kept and the *RMSE* was lowered. However, applying more extreme reduction (EPS-MOR-5p solutions) rised the *RMSE* and the number of remaining instances may be insufficient to train a model with sufficient generalization. And between these two (EPS-MOR-bsl solutions), a *RMSE* slightly lower than the baseline was achieved, but with higher compression values than EPS-MOR-1st solutions.

It is worth noting the results of data sets ATP1D and ENB, where the EPS-MOR-bsl solution, despite applying a reduction higher than EPS-MOR-1st, managed to reduce the *RMSE*. This effect could be explained because, although the solutions are from the Pareto front obtained in training, when the *RMSE* from the testing procedures was considered, the solutions themselves would not necessarily form a Pareto front.

As shown in subtables (b) and (c) of Tables 4, 5, and 6, the behavior of stacking and regressor chain were the same as in single target, shown in subtables (a) of the aforementioned tables. The solutions of the Pareto front in training appeared to form a Pareto

Table 6
Summary of the results for the *RMSE* with *k*-NN regressor with $k = 5$ (lower is better). The best result for each data set (and regressor) and the best values are highlighted in bold.

(a) Single-target

Data set	Original	EPS-MOR		
		1st	bsl	5pc
Andromeda	**0.5870**	0.6019	0.6019	0.6257
SCPF	0.7850	**0.7311**	0.7842	0.7971
Water quality	**0.7704**	0.7728	0.7728	0.7932
Solar flare 1	0.9539	**0.9044**	0.9072	0.9633
Solar flare 2	0.8868	**0.8423**	0.8606	0.8606
Slump	0.7121	**0.7098**	**0.7098**	0.7560
ATP1D	0.4435	**0.4412**	**0.4412**	0.4725
ATP7D	**0.6104**	0.6384	0.6384	0.6488
EDM	0.5812	**0.5701**	**0.5701**	0.6158
River flow 1	0.0876	**0.0758**	0.0874	0.0921
ENB	0.3123	**0.3032**	0.3065	0.3375
Jura	**0.7229**	0.7256	0.7256	0.7592
Online sales	0.8116	**0.8018**	**0.8018**	0.8603
Average	0.6358	**0.6245**	0.6313	0.6602

(b) Stacking of single-target

Data set	Original	EPS-MOR		
		1st	bsl	5pc
Andromeda	**0.5642**	0.5804	0.5804	0.6100
SCPF	0.7898	**0.7401**	0.7850	0.7965
Water quality	**0.7734**	0.7772	0.7772	0.8037
Solar flare 1	0.9892	**0.9068**	0.9186	0.9754
Solar flare 2	0.9058	**0.8618**	0.8739	0.8739
Slump	**0.7153**	0.7183	0.7183	0.7609
ATP1D	**0.4425**	0.4433	0.4433	0.4732
ATP7D	**0.6103**	0.6376	0.6376	0.6468
EDM	0.5841	**0.5701**	**0.5701**	0.6144
River flow 1	0.0813	**0.0769**	0.0882	0.0924
ENB	0.3110	**0.2997**	0.3076	0.3366
Jura	**0.7350**	0.7369	0.7369	0.7623
Online sales	0.8050	**0.8010**	**0.8010**	0.8769
Average	0.6390	**0.6269**	0.6337	0.6633

(c) chain of *k*-NN regressors

Data set	Original	EPS-MOR		
		1st	bsl	5pc
Andromeda	**0.5700**	0.6104	0.6104	0.6140
SCPF	0.7596	**0.7280**	0.7805	0.7854
Water quality	**0.7763**	0.7809	0.7809	0.7974
Solar flare 1	0.9562	**0.9065**	0.9086	0.9569
Solar flare 2	0.8890	**0.8459**	0.8559	0.8559
Slump	0.7273	**0.7211**	**0.7211**	0.7633
ATP1D	0.4422	**0.4418**	**0.4418**	0.4728
ATP7D	**0.6096**	0.6399	0.6399	0.6480
EDM	0.5840	**0.5701**	**0.5701**	0.6110
River flow 1	0.0875	**0.0757**	0.0875	0.0919
ENB	0.3091	**0.3057**	0.3072	0.3376
Jura	**0.7293**	0.7305	0.7305	0.7531
Online sales	0.8065	**0.8001**	**0.8001**	0.8499
Average	0.6344	**0.6274**	0.6334	0.6567

(d) ensemble of chains

Data set	Original	EPS-MOR		
		1st	bsl	5pc
Andromeda	**0.5999**	0.6212	0.6212	0.6282
SCPF	0.7374	**0.7306**	0.7540	0.7999
Water quality	**0.7627**	0.7662	0.7662	0.7692
Solar flare 1	0.9481	0.9087	**0.9049**	0.9630
Solar flare 2	0.8943	**0.8457**	0.8458	0.8458
Slump	0.7060	**0.7059**	**0.7059**	0.7426
ATP1D	**0.4322**	0.4383	0.4383	0.4637
ATP7D	**0.5999**	0.6436	0.6436	0.6415
EDM	**0.6344**	0.6755	0.6755	0.6843
River flow 1	**0.0791**	0.0793	0.0940	0.0980
ENB	0.3189	**0.3121**	0.3252	0.3541
Jura	**0.7247**	0.7348	0.7348	0.7679
Online sales	**0.7817**	0.7910	0.7910	0.8356
Average	**0.6322**	0.6348	0.6385	0.6611

Table 7
Summary of the compression results (in percentage) of the prototype selection method.

Data set	$k = 1$			$k = 3$			$k = 5$		
	1st	bsl	5pc	1st	bsl	5pc	1st	bsl	5pc
Andromeda	45.12	45.12	**49.29**	22.68	30.55	**40.74**	17.14	17.14	**17.80**
SCPF	67.99	**82.39**	**82.39**	67.16	83.18	**86.35**	67.62	75.20	**94.14**
Water quality	51.32	**80.86**	**80.86**	62.41	66.21	**80.31**	9.84	9.84	**81.08**
Solar flare 1	69.39	89.82	**95.51**	82.64	**89.65**	**89.65**	67.67	83.02	**89.48**
Solar flare 2	69.55	82.46	**82.97**	66.47	**78.85**	**78.85**	72.49	**82.85**	**82.85**
Slump	56.73	78.85	**80.05**	54.14	54.14	**56.31**	19.61	19.61	**63.73**
ATP1D	49.29	52.30	**59.94**	49.31	49.31	**60.15**	10.68	10.68	**57.91**
ATP7D	60.68	77.78	**79.67**	6.18	6.18	**59.62**	54.95	54.95	**56.24**
EDM	41.69	64.92	**67.76**	31.96	31.96	**52.29**	40.46	40.46	**46.62**
River flow 1	64.05	**79.32**	**79.32**	67.92	**73.88**	**73.88**	66.89	73.78	**76.16**
ENB	19.43	**80.86**	**80.86**	13.55	13.55	**14.02**	58.31	67.75	**80.91**
Jura	5.18	5.18	**62.39**	10.09	10.09	**57.02**	1.37	1.37	**48.29**
Online sales	9.93	44.71	**51.29**	5.52	5.52	**62.17**	10.33	10.33	**70.36**
Average	46.95	66.51	**73.25**	41.54	45.62	**62.41**	38.26	42.08	**66.58**

front for most training sets when the *RMSE* in the testing procedure was considered (except for data sets ATP1D and ENB mentioned as exceptions above).

The strategy of combining several regressors chains can be seen in subtables (d) of Tables 4, 5, and 6, corresponding to the regressor chain ensemble. As a robust ensemble method, the improvements introduced by prototype selection were hardly noticeable.

Table 7 shows the compression rates (in percentages) achieved by EPS-MOR when $k = 1$, $k = 3$ and $k = 5$ are used. As expected, the best compression rates were achieved at the point EPS-MOR-5pc (of the three selected solutions, which is towards the left) with an average compression rate of between 62 and 73%. Nevertheless, this high compression has as a counterpart high error rates, as has previously been shown. It should be mentioned that EPS-MOR-1st (the most conservative solution) achieved both high compression rates, of around $38 - 47\%$, and high accuracy expressed by a low *RMSE*.

5.3.1. Statistical tests

Average ranks [52] and the Hochberg procedure [53] were both computed for a proper comparison of the results. Table 8 summarizes the results of the *RMSE* for each regressor and *k* value for $k = 1$, 3, and 5. The best method according to the *RMSE* is highlighted in bold, and the symbol (✖) indicates that the result is statistically worse than the best method in each block (at a level of $\alpha = 0.05$).

Table 8
Average rankings for the different regressors and k values. The best results for each regressor and k value are highlighted in bold. The symbol (✖) marks the results that are statistically worse than the best in each block (at a level of $\alpha = 0.05$).

k value	Algorithm	Single-target	MT stacking	k-NN chain	Ensemble of chains
k= 1	Original	3.3077 ✖	3.3077 ✖	3.3846 ✖	2.5385
	EPS-MOR-1st	**1.3077**	**1.3077**	**1.3077**	**1.6145**
	EPS-MOR-bsl	1.9231	1.9231	1.9231	2.4615
	EPS-MOR-5pc	3.4615 ✖	3.4615 ✖	3.3846 ✖	3.3846 ✖
k= 3	Original	2.3077	2.0769	2.2308	2.2308
	EPS-MOR-1st	**1.8077**	**1.8846**	**1.8077**	**1.5709**
	EPS-MOR-bsl	2.2308	2.3846	2.3077	2.4615
	EPS-MOR-5pc	3.6538 ✖	3.6538 ✖	3.6538 ✖	3.7308 ✖
k = 5	Original	2.4615	2.1538	2.3846 ✖	**1.6923**
	EPS-MOR-1st	**1.6154**	**1.7692**	**1.6154**	2.0769
	EPS-MOR-bsl	2.0385	2.2692	2.1154	2.5000
	EPS-MOR-5pc	3.8846 ✖	3.8077 ✖	3.8846 ✖	3.7308 ✖

Table 9
Average rankings of compression. The best result for each regressor is highlighted in bold. The symbol (✖) marks the results that are statistically worse than the best (at a level of $\alpha = 0.05$).

Algorithm	$k = 1$	$k = 3$	$k = 5$
EPS-MOR-1st	2.9231 ✖	2.7308 ✖	2.6923 ✖
EPS-MOR-bsl	1.9231 ✖	2.1538 ✖	2.2692 ✖
EPS-MOR-5pc	**1.1538**	**1.1154**	**1.0385**

Some remarks of interest in relation to Table 9 are as follows:

- The subsets obtained with EPS-MOR-1st consistently yielded the best results in all situations, except in the case of the ensemble of chains of regressors at $k = 5$. As previously discussed, the robustness obtained by the ensemble and a high number of k had already yielded a very good result that would be difficult to improve upon.
- If we focus on the value of the regressors with $k = 1$, the solutions corresponding to EPS-MOR-1st were significantly better than those obtained when using the whole data set, for all methods, except, once again, for the ensemble of chains of regressors, where it was better (but not significantly).
- For all regressors and k values, EPS-MOR-1st was significantly better than EPS-MOR-5pc. As commented earlier, the compression of EPS-MOR-5pc was too high and the highly reduced data sets were unable to retain the prediction capabilities of the whole data set.

Table 9 shows the Average ranks and Hochberg procedures over compression. As expected, taking into account compression, the best results were achieved by EPS-MOR-5pc, followed by EPS-MOR-bsl and EPS-MOR-1st, in that order. Moreover, the differences between EPS-MOR-5pc and the other two were significant (at a level of $\alpha = 0.05$).

6. Conclusions

EPS-MOR has been presented as the first prototype selection method for multi-output regression problems. The bi-objective evolutionary algorithm NSGA-II has been used as the search algorithm for the prototype selection method. The design of EPS-MOR overcomes the limitations of the NSGA-II regarding overfitting by using, when needed, more than one Pareto front with specific initialization and mutation parameters, which were merged to obtain the final solutions. Also, to speed up the evaluation of the fitness function, the distances were pre-calculated and cached at the beginning of the execution.

The experimental validation of EPS-MOR has shown that despite the large reduction of data set size, in some cases by more than 50%, when the selected instances are used to train multi-output regressors, their performance is not worse and can even be better than having trained the regressors on the whole data set.

The performance and efficiency shown by EPS-MOR demonstrates that the Pareto-based multi-objective evolutionary approach can offer a good trade-off between compression and accuracy for multi-output regression tasks. One of its great advantages is that, instead of a single solution, many solutions are obtained from which one can be chosen. So, if greater importance is attached to the reduction of the *RMSE*, a solution on the right side of the Pareto front can be used. Otherwise, if the reduction of the data set size is being sought, a left side solution can be chosen.

Declaration of competing interest

We declare that there is no conflict of interest.

Acknowledgements

This work was supported by the NCN (Polish National Science Center) grant "*Evolutionary Methods in Data Selection*" No. 2017/01/X/ST6/00202, project TIN2015-67534-P (MINECO/FEDER, UE) of the *Ministerio de Economía y Competitividad* of the Spanish Government, and project BU085P17 (JCyL/FEDER, UE) of the *Junta de Castilla y León* cofinanced with European Union FEDER funds.

References

[1] G. Tsoumakas, I. Katakis, Multi-label classification: an overview, Int. J. Data Warehous. Mining 3 (3) (2007) 1–13.
[2] H. Borchani, G. Varando, C. Bielza, P. Larrañaga, A survey on multi-output regression, Wiley Interdiscipl. Rev.: Data Mining Knowl. Discov. 5 (5) (2015) 216–233, doi:10.1002/widm.1157.
[3] A. de Haro-García, J. Pérez-Rodríguez, N. García-Pedrajas, Combining three strategies for evolutionary instance selection for instance-based learning, swarm and evolutionary computation, doi:10.1016/j.swevo.2018.02.022.
[4] D.R. Wilson, T.R. Martinez, Reduction techniques for instance-based learning algorithms, Mach. Learn. 38 (3) (2000) 257–286, doi:10.1023/A:1007626913721.
[5] S. Garcia, J. Derrac, J. Cano, F. Herrera, Prototype selection for nearest neighbor classification: Taxonomy and empirical study, IEEE Trans. Pattern Anal. Mach. Intell. 34 (3) (2012) 417–435, doi:10.1109/TPAMI.2011.142.
[6] M. Kordos, M. Blachnik, Instance selection with neural networks for regression problems, in: Artificial Neural Networks and Machine Learning - ICANN 2012, Vol. 7553 of Lecture Notes in Computer Science, Springer Berlin Heidelberg, 2012, pp. 263–270, doi:10.1007/978-3-642-33266-1_33.
[7] A. Arnaiz-González, J.F. Díez-Pastor, J.J. Rodríguez, C.I. García-Osorio, Instance selection for regression: Adapting DROP, Neurocomputing 201 (2016a) 66–81, doi:10.1016/j.neucom.2016.04.003.
[8] A. Arnaiz-González, J.F. Díez-Pastor, J.J. Rodríguez, C. García-Osorio, Instance selection of linear complexity for big data, Knowl.-Based Syst. 107 (2016b) 83–95, doi:10.1016/j.knosys.2016.05.056.
[9] A. Arnaiz-González, A. González-Rogel, J.F. Díez-Pastor, C. López-Nozal, MR-DIS: democratic instance selection for big data by MapReduce, Progr. Artif. Intell. 6 (3) (2017) 211–219, doi:10.1007/s13748-017-0117-5.
[10] S. Ramírez-Gallego, B. Krawczyk, S. García, M. Woźniak, J.M. Benítez, F. Herrera, Nearest neighbor classification for high-speed big data streams using spark, IEEE Trans. Syst. Man Cybern.: Syst. 47 (10) (2017) 2727–2739, doi:10.1109/TSMC.2017.2700889.
[11] A. Arnaiz-González, J.F. Díez-Pastor, J.J. Rodríguez, C.I. García-Osorio, Study of data transformation techniques for adapting single-label prototype selection algorithms to multi-label learning, Expert Syst. Appl. 109 (2018) 114–130, doi:10.1016/j.eswa.2018.05.017.

[12] K. Deb, A. Pratap, S. Agarwal, T. Meyarivan, A fast and elitist multiobjective genetic algorithm: NSGA-II, IEEE Trans. Evolut. Comput. 6 (2) (2002) 182–197, doi:10.1109/4235.996017.
[13] E. Spyromitros-Xioufis, G. Tsoumakas, W. Groves, I. Vlahavas, Multi-target regression via input space expansion: treating targets as inputs, Mach. Learn. 104 (1) (2016) 55–98, doi:10.1007/s10994-016-5546-z.
[14] E. Spyromitros-Xioufis, W. Groves, G. Tsoumakas, I.P. Vlahavas, Multi-label classification methods for multi-target regression, CoRR (2012) http://arxiv.org/abs/1211.6581.
[15] T. Aho, B. Ženko, S. Džeroski, T. Elomaa, Multi-target regression with rule ensembles, J. Mach. Learn. Res. 13 (2012) 2367–2407.
[16] Z. Han, Y. Liu, J. Zhao, W. Wang, Real time prediction for converter gas tank levels based on multi-output least square support vector regressor, Control Eng. Pract. 20 (12) (2012) 1400–1409, doi:10.1016/j.conengprac.2012.08.006.
[17] D. Kocev, S. Džeroski, M.D. White, G.R. Newell, P. Griffioen, Using single- and multi-target regression trees and ensembles to model a compound index of vegetation condition, Ecol. Model. 220 (8) (2009) 1159–1168, doi:10.1016/j.ecolmodel.2009.01.037.
[18] G. Tsoumakas, E. Spyromitros-Xioufis, J. Vilcek, I. Vlahavas, Mulan: a java library for multi-label learning, J. Mach. Learn. Res. 12 (2011) 2411–2414.
[19] O. Luaces, J. Díez, J. Barranquero, J.J. del Coz, A. Bahamonde, Binary relevance efficacy for multilabel classification, Progr. Artif. Intell. 1 (4) (2012) 303–313, doi:10.1007/s13748-012-0030-x.
[20] S. Godbole, S. Sarawagi, Discriminative methods for multi-labeled classification, in: H. Dai, R. Srikant, C. Zhang (Eds.), Advances in Knowledge Discovery and Data Mining, Springer Berlin Heidelberg, Berlin, Heidelberg, 2004, pp. 22–30.
[21] J. Read, B. Pfahringer, G. Holmes, E. Frank, Classifier chains for multi-label classification, Mach. Learn. 85 (3) (2011) 333, doi:10.1007/s10994-011-5256-5.
[22] H. Brighton, C. Mellish, Advances in instance selection for instance-based learning algorithms, Data Mining Knowl. Discov. 6 (2) (2002) 153–172, doi:10.1023/A:1014043630878.
[23] J.A. Olvera-López, J.A. Carrasco-Ochoa, J.F. Martínez-Trinidad, J. Kittler, A review of instance selection methods, Artif. Intell. Rev. 34 (2) (2010) 133–143, doi:10.1007/s10462-010-9165-y.
[24] E. Leyva, A. González, R. Pérez, Three new instance selection methods based on local sets: a comparative study with several approaches from a bi-objective perspective, Pattern Recognit. 48 (4) (2015) 1523–1537, doi:10.1016/j.patcog.2014.10.001.
[25] P. Hart, The condensed nearest neighbor rule (corresp.), IEEE Trans. Inf. Theory 14 (3) (1968) 515–516.
[26] D.L. Wilson, Asymptotic properties of nearest neighbor rules using edited data, IEEE transactions on systems, Man Cybern. SMC 2 (3) (1972) 408–421, doi:10.1109/TSMC.1972.4309137.
[27] M. Rahmani, G. Atia, Robust and scalable column/row sampling from corrupted big data, in: Proceedings of the 2017 IEEE International Conference on Computer Vision Workshops (ICCVW), 2017, pp. 1818–1826, doi:10.1109/ICCVW.2017.215.
[28] E. Elhamifar, G. Sapiro, S.S. Sastry, Dissimilarity-based sparse subset selection, IEEE Trans. Pattern Anal. Mach. Intell. 38 (11) (2016) 2182–2197, doi:10.1109/TPAMI.2015.2511748.
[29] E. Elhamifar, G. Sapiro, R. Vidal, See all by looking at a few: Sparse modeling for finding representative objects, in: Proceedings of the IEEE Conference on Computer Vision and Pattern Recognition, 2012a, pp. 1600–1607, doi:10.1109/CVPR.2012.6247852.
[30] E. Elhamifar, G. Sapiro, R. Vidal, Finding exemplars from pairwise dissimilarities via simultaneous sparse recovery, in: F. Pereira, C.J.C. Burges, L. Bottou, K.Q. Weinberger (Eds.), Advances in Neural Information Processing Systems 25, Curran Associates, Inc., 2012b, pp. 19–27.
[31] B.J. Frey, D. Dueck, Clustering by passing messages between data points, Science 315 (5814) (2007) 972–976, doi:10.1126/science.1136800.
[32] J. Derrac, S. García, F. Herrera, A survey on evolutionary instance selection and generation, in: Modeling, Analysis, and Applications in Metaheuristic Computing: Advancements and Trends, IGI Global, 2012, pp. 233–266.
[33] N. García-Pedrajas, A. de Haro-García, J. Pérez-Rodríguez, A scalable approach to simultaneous evolutionary instance and feature selection, Inf. Sci. 228 (2013) 150–174, doi:10.1016/j.ins.2012.10.006.
[34] L.I. Kuncheva, Editing for the k-nearest neighbors rule by a genetic algorithm, Pattern Recognit. Lett. 16 (8) (1995) 809–814, doi:10.1016/0167-8655(95)00047-K. Genetic Algorithms.
[35] J.R. Cano, F. Herrera, M. Lozano, Using evolutionary algorithms as instance selection for data reduction in KDD: an experimental study, IEEE Trans. Evolut. Comput. 7 (6) (2003) 561–575, doi:10.1109/TEVC.2003.819265.
[36] J. Tolvi, Genetic algorithms for outlier detection and variable selection in linear regression models, Soft Comput. 8 (8) (2004) 527–533, doi:10.1007/s00500-003-0310-2.
[37] N. García-Pedrajas, J.A.R. del Castillo, D. Ortiz-Boyer, A cooperative coevolutionary algorithm for instance selection for instance-based learning, Mach. Learn. 78 (3) (2010) 381–420, doi:10.1007/s10994-009-5161-3.
[38] M. Antonelli, P. Ducange, M. F., Genetic training instance selection in multiobjective evolutionary fuzzy systems: a coevolutionary approach, IEEE Trans. Fuzzy Syst. 20 (2) (2012) 276–290, doi:10.1109/TFUZZ.2011.2173582.
[39] A. Rosales-Pérez, S. García, J.A. Gonzalez, C.A.C. Coello, F. Herrera, An evolutionary multiobjective model and instance selection for support vector machines with pareto-based ensembles, IEEE Trans. Evolut. Comput. 21 (6) (2017) 863–877, doi:10.1109/TEVC.2017.2688863.
[40] H.J. Escalante, M. Marin-Castro, A. Morales-Reyes, M. Graff, A. Rosales-Pérez, M.M.-y. Gómez, C.A. Reyes, J.A. Gonzalez, MOPG: a multi-objective evolutionary algorithm for prototype generation, Pattern Anal. Appl. 20 (1) (2017) 33–47, doi:10.1007/s10044-015-0454-6.
[41] G. Acampora, F. Herrera, G. Tortora, A. Vitiello, A multi-objective evolutionary approach to training set selection for support vector machine, Knowl.-Based Syst. 147 (2018) 94–108, doi:10.1016/j.knosys.2018.02.022.
[42] D.W. Corne, N.R. Jerram, J.D. Knowles, M.J. Oates, PESA-II: region-based selection in evolutionary multiobjective optimization, in: Proceedings of the 3rd Annual Conference on Genetic and Evolutionary Computation, GECCO'01, Morgan Kaufmann Publishers Inc., San Francisco, CA, USA, 2001, pp. 283–290.
[43] F. Charte, A.J. Rivera, M.J. del Jesus, F. Herrera, MLeNN: a first approach to heuristic multilabel undersampling, in: Proceedings of the : 15th International Conference Intelligent Data Engineering and Automated Learning – IDEAL 2014, Springer International Publishing, Salamanca, Spain, 2014, pp. 1–9, doi:10.1007/978-3-319-10840-7_1. September 10–12, 2014. Proceedings.
[44] S. Kanj, F. Abdallah, T. Denœux, K. Tout, Editing training data for multi-label classification with the k-nearest neighbor rule, Pattern Anal. Appl. 19 (1) (2016) 145–161, doi:10.1007/s10044-015-0452-8.
[45] A. Arnaiz-González, J.F. Díez-Pastor, J.J. Rodríguez, C.I. García-Osorio, Local sets for multi-label instance selection, Appl. Soft Comput. doi:10.1016/j.asoc.2018.04.016.
[46] H. Brighton, C. Mellish, On the Consistency of Information Filters for Lazy Learning Algorithms, Springer Berlin Heidelberg, Berlin, Heidelberg, 1999, pp. 283–288, doi:10.1007/978-3-540-48247-5_31.
[47] R.T. Marler, J.S. Arora, Survey of multi-objective optimization methods for engineering, Struct. Multidiscipl. Optim. 26 (6) (2004) 369–395.
[48] W.K. Mashwant, Enhanced versions of differential evolution: state-of-the-art survey, Int. J. Comput. Sci. Math. 5 (2) (2014) 107–126.
[49] K. Deb, Multi-Objective Optimization Using Evolutionary Algorithms, Wiley, 2009.
[50] Y. Yuan, H. Xu, B. Wang, An improved NSGA-III procedure for evolutionary many-objective optimization, in: Proceedings of the 2014 Annual Conference on Genetic and Evolutionary Computation, GECCO '14, ACM, New York, NY, USA, 2014, pp. 661–668, doi:10.1145/2576768.2598342.
[51] I.H. Witten, E. Frank, M.A. Hall, Data Mining: Practical Machine Learning Tools and Techniques, 3rd, Morgan Kaufmann Publishers Inc., San Francisco, CA, USA, 2011.
[52] J. Demšar, Statistical comparisons of classifiers over multiple data sets, J. Mach. Learn. Res. 7 (2006) 1–30.
[53] Y. Hochberg, A sharper Bonferroni procedure for multiple tests of significance, Biometrika 75 (4) (1988) 800–802, doi:10.1093/biomet/75.4.800.

Mirosław Kordos obtained M.Sc. in electrical engineering from Technical University of Lodz, Poland in 1994 and Ph.D. in computer science from Silesian University of Technology, Poland in 2005. In years 1994–2005 he was working in IT industry as software developer and systems engineer. In 2006–2007 he was a research fellow at the Division of Biomedical Informatics in Cincinnati Children's Hospital Research Center, USA. In 2008–2009 he was an assistant professor at Silesian University of Technology, Poland and since 2010 he is an assistant professor at University of Bielsko-Biala, Poland. His research interest in recent years is mainly focused on instance selection in machine learning with classical methods, evolutionary methods and methods embedded into neural networks. He is an author or co-author of over 20 papers on instance selection.

Álvar Arnaiz González received his M.S. degree in Computer Engineering in 2010, and the Ph.D. in Computer Science in 2018 at the University of Burgos, Spain, for a thesis entitled "Study of instance selection methods". He is currently an Assistant Professor at the Department of Civil Engineer of the Burgos University. His main research interests include Machine Learning, Data Mining, ensemble classifiers and instance selection. He is a member of the "Artificial Data Mining Research and Bioinformatics Learning" research group.

César García-Osorio was born in León, Spain. He received his B.S. and M.E. in Computer Engineering in 1996 at the University of Valladolid, Spain, and the PhD in Computer Science in 2005 at the University of the West of Scotland, United Kingdom, for a thesis entitled "Data mining and visualization". He has been working at University of Burgos since 1996. His research interests include among others, ensemble learning, instance selection, data visualization. He is a member of the "Artificial Data Mining Research and Bioinformatics Learning" research group.